

UNIVERSITAT POLITÈCNICA DE CATALUNYA

Barcelona East School of Engineering

Master's degree in Interdisciplinary and Innovative Engineering

HUMAN ACTIVITY DETECTION BASED ON MOBILE DEVICES



Report and Annexes

Author: Shiyang Li
Director: Jordi Cosp Vilella
Convocatoria: Jun 2022

Abstract

This thesis focuses on human activity detection based on mobile and wearable devices. We choose Hexiwear as our wearable device to collect the human daily activity data, like tri-axis acceleration, tri-axis orientation, tri-axis angular velocity and position. This project consists in the development of a smartphone application for the user in data analysis, data visualization and generates results. The objective is to build an open and modular prototype that can serve as an example or template for the development of other projects. The application is developed using JAVA by Android Studio. The application allows the user to connect with the wearable device, and recognize their daily activity. For the daily activity classify algorithm, we used two different methods, the first one is by set different thresholds, the second is by using the machine learning. The application was tested and the results were satisfactory, as the generated application worked properly. Despite the obvious limitations, the work done is a starting point for future developments.

Resum

Aquesta tesi se centra en la detecció d'activitat humana a partir de dispositius mòbils i portàtils. Escollim Hexiwear com el nostre dispositiu portàtil per recollir les dades de l'activitat humana diària, com ara l'acceleració de tres eixos, l'orientació de tres eixos, la velocitat angular i la posició de tres eixos. Aquest projecte consisteix en el desenvolupament d'una aplicació per a telèfon intel·ligent per a l'usuari en l'anàlisi de dades, la visualització de dades i la generació de resultats. L'objectiu és construir un prototip obert i modular que pugui servir d'exemple o plantilla per al desenvolupament d'altres projectes. L'aplicació està desenvolupada amb JAVA per Android Studio. L'aplicació permet a l'usuari connectar-se amb el dispositiu portàtil i reconèixer la seva activitat diària. Per a l'algorisme de classificació de l'activitat diària, hem utilitzat dos mètodes diferents, el primer és mitjançant l'establiment de diferents llindars, el segon és mitjançant l'aprenentatge automàtic. L'aplicació es va provar i els resultats van ser satisfactoris, ja que l'aplicació generada va funcionar correctament. Malgrat les òbvies limitacions, la feina feta és un punt de partida per a desenvolupaments futurs.

Resumen

Esta tesis se centra en la detección de actividad humana basada en dispositivos móviles y portátiles. Elegimos Hexiwear como nuestro dispositivo portátil para recopilar los datos de la actividad humana diaria, como la aceleración de tres ejes, la orientación de tres ejes, la velocidad angular de tres ejes y la posición. Este proyecto implica la creación de una aplicación de teléfono para usuarios de análisis de datos, visualización de datos y generación de resultados. El objetivo es construir un prototipo abierto y modular que pueda servir como ejemplo o plantilla para el desarrollo de otros proyectos. La aplicación está desarrollada usando JAVA por Android Studio. La aplicación permite al usuario conectarse con el dispositivo portátil y reconocer su actividad diaria. Para el algoritmo de clasificación de la actividad diaria, usamos dos métodos diferentes, el primero es establecer umbrales diferentes, el segundo es usar el aprendizaje automático. La aplicación fue probada y los resultados fueron satisfactorios, ya que la aplicación generada funcionó correctamente. A pesar de las limitaciones evidentes, el trabajo realizado es un punto de partida para futuros desarrollos.

Acknowledgment

First and foremost, I would like to thank my tutor Dr. Cosp-Vilella, for the amount of time he spent helping me and guiding me through this project. Because of this project, I have found a direction that I want to continue my research in the future. Secondly, I would like to thank the faculty of Interdisciplinary and Innovative Engineering for the knowledge and experience I have gained during these two years of study. And I would like to thank Raul Benitez, who has been a constant source of help since I started at UPC. Many thanks to my family for their unconditional support, without them I would not have been able to finish.

Glossary

HAR – Human Activity Recognition

UPDRS – Unified Parkinson’s Disease Rating Scale

CDC – Centers for Disease Control

IOT – Internet of Things

BLE – Bluetooth Low Energy

PHY – Physical Layer

LL – Link Layer

HC – Host-Control interface layer

L2CAP – Host mainly includes the logical Link Control and Adaption Protocol later

SM – Security Manager

ATT – Attribute Protocol

GAP – Generic Access Profile

AHRS – Attitude and Heading Reference Systems

IMU – Inertial Measurement Units

RMS – Root Mean Square

Index

ABSTRACT	I
RESUM	II
RESUMEN	III
ACKNOWLEDGMENT	IV
GLOSSARY	V
LIST OF FIGURES	IX
LIST OF TABLE	XI
1. PREFACE	13
1.2. Project origin and motivation.....	13
1.3. Project Goals & Scope	13
2. INTRODUCTION	14
2.1. Background	14
2.2. Human daily activity	15
3. AVAILABLE TECHNOLOGIES AND CHOSEN SOLUTION	17
3.1. Wearable devices.....	17
3.1.1. Hexiwear	18
3.1.2. Xsens Dot.....	19
3.1.3. Blue Trident.....	19
3.2. Operating systems	20
3.2.1. Android Operating System.....	21
3.2.2. iOS Operating System	21
3.3. Reason for chosen	22
3.3.1. Overall scheme.....	22
3.3.2. Hardware.....	23
3.3.3. Software	24
4. THEORETICAL BACKGROUND	27
4.1. Wireless communication	27
4.1.1. Low Energy Bluetooth 4.0 Overview	27
4.1.2. Low Energy Bluetooth 4.0 protocol stack.....	27
4.1.3. Compare several short-range Wireless communication technologies	28

4.2.	Orientation	29
4.2.1.	Represent Orientation.....	29
4.2.2.	Measure of Orientation.....	32
5.	IMPLEMENTATION	36
5.1.	Devices connect	36
5.2.	Data collection	37
5.2.1.	Data collection.....	37
5.2.2.	Sample frequency.....	37
5.3.	Data treatment	38
5.3.1.	Data import.....	38
5.3.2.	Madgwick algorithm.....	38
5.3.3.	Calculate Euler angles.....	39
5.3.4.	Gravity compensation	39
5.4.	Data analysis	39
5.4.1.	Feature Extraction	39
5.4.2.	Feature selection	40
5.5.	Experimental procedure	41
6.	RESULTS	44
6.1.	Horizontal Activity.....	45
6.2.	Vertical Activity	46
6.3.	Final Results.....	48
7.	CONCLUSIONS	50
7.1.	Summary	50
7.2.	Proposal and future work	50
8.	ECONOMIC STUDY	51



List of Figures

Figure 2.1. Human daily activity	15
Figure 3.1. Wearable unit shipments worldwide from 2014 to 2021 (source: Statista)	17
Figure 3.2. Hexiwaer device (source: MikroElektronika)	18
Figure 3.3. Xsens Dot device (source: Xsens.com [33])	19
Figure 3.4. Operating System (source: statcounter)	21
Figure 3.5. (a), (b) Hexiwear's PCB; (c) Hardware's block diagram. (source: MikroElektronika)	24
Figure 3.6. Android Studio Log (source: android.com)	25
Figure 4.1. Low Energy Bluetooth Protocol Stack (source: Bluetooth Low Energy Software Developer's Guide)	27
Figure 4.2. Hexiwear orientation and axis orientation (source: MikroElektronika)	29
Figure 4.3. Tait-Bryan angles in Z-Y-X sequence (source: Yusheng [44])	30
Figure 4.4. Madgwick's algorithm block diagram structure (source: madgwick internal report [39])	34
Figure 5.1. The block diagram of Algorithm	36
Figure 5.2. Sensors used for measurement: FXOS8700CQ, FXAS21002 (source: MikroElektronika)	37
Figure 5.3. Data treatment block diagram.	38
Figure 5.4. Raw data from Hexiwear.	38
Figure 5.5. The framework of experimental procedure.	41
Figure 5.6. Screen to search for Bluetooth.	42

Figure 5.7. Screen to connect device.	43
Figure 5.8. Screen of results.	43
Figure 6.1. Classification of human daily activities.	44
Figure 6.2. Plot the standing and sitting data from 3 different sensor of Hexiwear.	45
Figure 6.3. Plot the lying data from 3 different sensor of Hexiwear.	45
Figure 6.4. Plot the running data from 3 different sensor of Hexiwear.	46
Figure 6.5. Plot the walking data from 3 different sensor of Hexiwear.	46
Figure 6.6. Plot the falling data from 3 different sensor of Hexiwear.	47

List of Table

Table 3.1 Hexiwear Sensor Characteristics	18
Table 3.2 Performance comparison of smartphone and Hexiwear	22
Table 4.1 Compare several wireless communication technologies	28
Table 5.1 Feature description	40
Table 6.1 Experiment results	48
Table 8.1 Cost of materials and licenses	51
Table 8.2 Total cost of project	51

1. PREFACE

1.2. Project origin and motivation

The origin of this project comes from the wearable devices final course project. However, in the course final project, we only collect human activity data through the built-in sensor of the mobile phone and upload the data to MATLAB for pre-processing and analysis. A complete activity recognition system is not implemented.

At the same time, the recording of human activity is becoming increasingly important in detecting activity in public health care. In our daily life, a reliable human activity recording system can not only encourage people to exercise more outdoors, but also can evaluate activities of daily living. for chronic treatment. It helps medical staff to come up with more reliable treatment options. Second, with the popularity of smart devices, people are more interested in wearing simple and comfortable devices to record their daily activity data all the time.

Thus, in this final project, we are going to build a complete human activity recognition system. According to Dr. Cosp-Vilella, the proposed project could be the focus of a final master's thesis (TFM), as the student could contribute the knowledge they have learned throughout their master's degree and in their chosen medical field to help develop an algorithm that could define various human activities.

1.3. Project Goals & Scope

The goal is to provide a functional prototype application. The application is aimed at simplicity prioritizing ease of use. It is designed to be multiplatform, easy to install and portable, so the users can easily set it up and access it directly. The object and scope of this project includes several points:

- Enables wireless communication between wearable device and smartphone.
- Find a suitable algorithm and embedded in our application.
- Result visualization

2. INTRODUCTION

2.1. Background

Wearable electronic technology integrates electronic devices with the human body in the form of clothing, accessories, skin patches, and in-vivo implantation, and realizes functions such as in-body sensing measurement, data storage, and mobile computing. An important part of wearable systems is wearable sensors with varied functions, that became highly regarded in industrial, medical, military, recreation and alternative fields in recent years. They can be used to evaluate many physiological parameters of the human body, such as observe the patient's body temperature, brain activity, heart rate, muscle motion and alternative key information [10], [11], and can also be used to measure various movements of the human body Status, such as acceleration, muscle extension, and foot pressure. They can also measure environment-related parameters, such as location coordinates, temperature, humidity, and atmospheric pressure.

The integration of wearable sensors and medical treatment can give patients with a more tailored treatment plan, as well as allow doctors to grasp the patient's recovery situation in real time, change and optimize the treatment plan in real time for various treatment problems, and accomplish accurate and quantitative therapy. Wearable sensors can also give large data support for the study of many complex diseases as well as data support for the attribution of different diseases brought on by environmental factors, dietary preferences, and individual differences. Wearable sensors have been applied to a variety of disease monitoring, which can be used not only as a preventive measure for sudden diseases [12],[13], but also as an adjuvant treatment and monitoring method in disease rehabilitation [14],[15],[16].

Take Parkinson's disease, for example. Parkinson's disease is a common neurodegenerative disease affecting about 3% of the global population over the age of 65 [17]. The Unified Parkinson's Disease Rating Scale is the primary evaluation tool used to assess the effectiveness of pharmacological and surgical combinations in the treatment of Parkinson's disease (UPDRS). comprehensive assessment of motor characteristics including finger and hand motions, posture, gait, hands and feet, and limbs. The use of wearable sensors makes it potential for patients when the onset of unwellness comparable to Parkinson's disease to hold out necessary treatment reception [18],[19],[20]. In recent years, the rapid development of gait analysis systems based on wearable accelerometers and gyroscopes has contributed greatly to more convenient and continuous monitoring of the gait of Parkinson's patients. These new systems not only make it easier and more direct to measure standard gait parameters and analyze related data, but also provide the ability to grade Parkinson's disease stage and degree of

dyskinesia. Klucken et al. [21] used shoes with integrated acceleration sensors and gyroscopes to record motion signals in standard gait sequences, and applied a large number of sensors feature signals (more than 650) and pattern recognition algorithms to classify Parkinson's disease stages. By comparing the results of sensor acquisition and analysis with Parkinson's clinical evaluation indicators (such as UPDRS part III exercise indicators), it is found that the classification accuracy of the wearable monitoring system reaches 81% to 91%.

Similarly, fall detection is also the current research direction of wearable sensors. The world is dealing with an getting old population. With this growth, the percentage of frail and established older adults might also additionally moreover growth considerably [22]. This demographic shift can cause an exponential increase within the variety of older adults gashed by falls, as falls and fall-related fractures are quite common among older adults. According to the Centers for Disease Control and Prevention (CDC), accidental falls are common among older adults, affecting approximately 30% of those > 65 years of age each year [23]. Older adults are at the highest risk of death or serious injury from falls, and also the risk will increase with age [24].

In this paper, we design a system capable of detecting human activity in real time and capable of detecting falls. A prototype system is implemented using Hexiwear and Android software, and the real-time data is verified by MATLAB.

2.2. Human daily activity

The human daily activity can be roughly divided into dynamic activities and static activities. Dynamic activities can be divided into cyclic or non-cyclic activities, and static activities are mainly divided into sitting, lying, and standing.

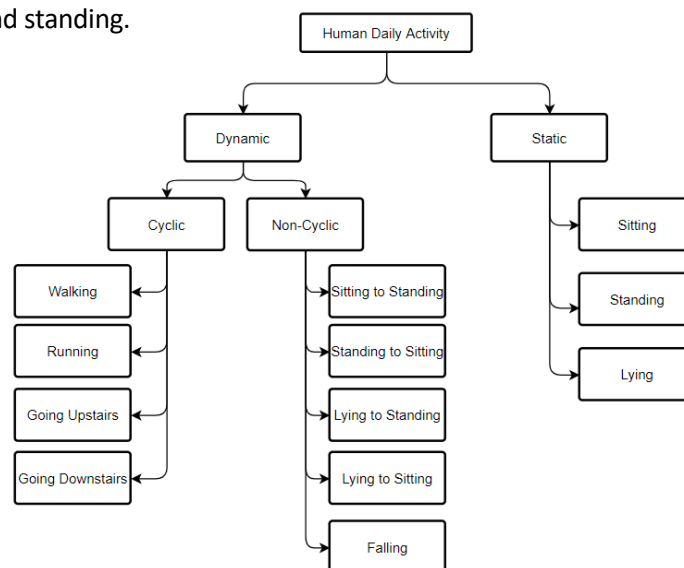


Figure 2.1. Human daily activity

Human activity recognition based on sensors has been studied for a long time. For example, KASTERENT V et al identify various human activities indoors by arranging sensor networks indoors [25]. RAVI N et al used a single three-axis accelerometer to identify 9 motion states such as standing, running, brushing teeth with good results [26]. CASALE P et al proposes that based on a single acceleration sensor system, five motion states can be recognized, and the recognition accuracy rate reaches 94%. KHAN proposes a hierarchical prediction model to classify the static, dynamic and excessive activities of the human body, which can identify 15 kinds of activities of the human body [28].

This paper uses Hexiwear's built-in sensors, including accelerometers, magnetometers and gyroscopes, to identify 5 common motion states in daily life.

3. AVAILABLE TECHNOLOGIES AND CHOSEN SOLUTION

3.1. Wearable devices

Devices that can be worn outside of clothing or on the body are known as wearables. capable of carrying out a number of the duties and features carried out by smartphones, laptops, and tablets. They can also carry out tasks more easily and effectively than portable and hand-held gadgets. When it comes to sensory feedback and causal abilities, they frequently exhibit a great deal of subtlety. The more vital is that offer feedback communications of permit the user to look at or access info in real time.

At present, wearable devices in the market are mainly concentrated in three major areas, namely, recreation, fitness, and medical health. From the table below we can find that wearable device shipments have increased significantly since 2018. 2021 global wearable device shipments are 533.6 million units. This is a 20% year-on-year increase, indicating that people are increasingly dependent on wearable devices.

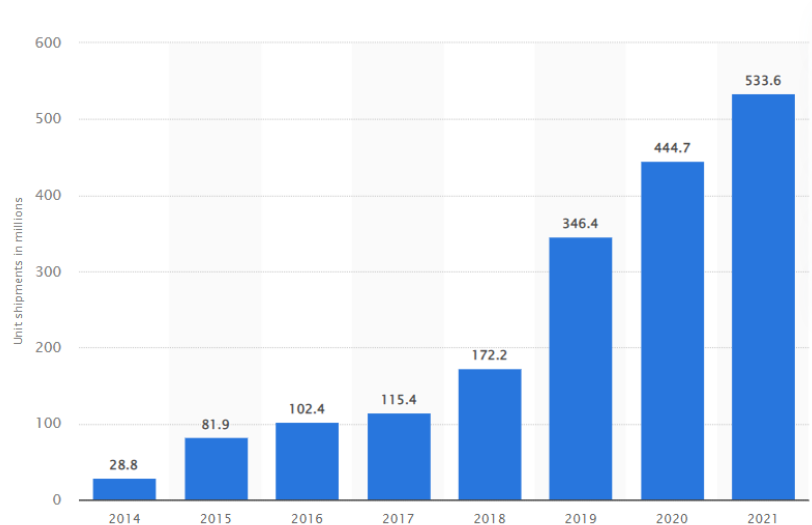


Figure 3.1. Wearable unit shipments worldwide from 2014 to 2021 (source: Statista)

In this project, a wearable device prototype with many sensors to test and develop applications or other devices is presented. Several alternatives are discussed in the section that follows.

3.1.1. Hexiwear

Hexiwear could be a wearable development kit for the net of Things (IoT). It is a small and energy-green device, filled with sensors to quantify ourselves or the sector around. It is wirelessly enabled and connect to both nearby devices or cloud servers far away. Its best feature is going to be the new and original software that we are going to develop. Hexiwear is powered by a kinetic 32-bit arm cortex-m for microcontroller. It has Bluetooth Low Energy and accelerometer, sensors for measuring altitude, light, heart rates and on the outside of full colored LED display.



Figure 3.2. Hexiwaer device (source: MikroElektronika)

Hexiwear provides BLE (Bluetooth Low Energy) for wireless communications, and consist of several sensors:

Table 3.1 Hexiwear Sensor Characteristics

Sensor:	Accelerometer	Magnetometer	Gyroscope
Sample frequency	Up to 800 Hz	Up to 800 Hz	Up to 800 Hz
Range	± 2 g, ± 4 g, ± 8 g	± 1200 μ T	$\pm 250^\circ$ /s, $\pm 500^\circ$ /s, $\pm 1000^\circ$ /s, $\pm 2000^\circ$ /s
Sensitivity	16-bit	16-bit	16-bit

3.1.2. Xsens Dot

Xsens Dot is a wearable sensor. It consists of 3D accelerometer, magnetometer and gyroscope. The embedded processor within the device handles sampling, calibration, strap-integration of mechanical phenomenon data and also the Xsens Kalman Filter core formula for sensor fusion. Xsens Dot can offer real-time 3D orientation likewise as mark 3D linear acceleration, angular velocity and magnetic field data to receiving device by Bluetooth 5.0[33].



Figure 3.3. Xsens Dot device (source: Xsens.com [33])

- Gyroscope
 - Sample frequency: 800 Hz
 - Range: $\pm 2000^\circ/\text{s}$
 - Sensitivity: 16-bit
- Accelerometer
 - Sample frequency: 800 Hz
 - Range: ± 16 g
 - Sensitivity: 16-bit
- Magnetometer
 - Sample frequency: 60 Hz
 - Range: ± 8 gauss
 - Sensitivity: 16-bit

3.1.3. Blue Trident

Blue Trident is a human motion capture device. It is ideal to be used with running based mostly sport, together with basketball, rugby, and football, aboard cricket, swimming and more. Embody a dual-g IMU, which may capture up to two hundred g. The low g sensor tracks lower intensity movements at

sixteen g and each sensors live movement simultaneously, guaranteeing accurate information capture, eliminating sensor saturation. The data download is very fast, one-hour capture takes three minutes. It has small volume and efficient battery, battery life up to 12 hours [34].



Figure 3.4. Blue Trident device (source: Vicon.com [34])

- Accelerometer
 - Sample frequency: 1125-1600 Hz
 - Range: $\pm 16g$, $\pm 200g$
 - Sensitivity: 16-bit, 13-bit
- Gyroscope
 - Sample frequency: 1125Hz
 - Range: $\pm 2000^\circ/s$
 - Sensitivity: 16-bit
- Magnetometer
 - Sample frequency: 1125Hz
 - Range: $\pm 4900 \mu T$
 - Sensitivity: 16-bit

3.2. Operating systems

In our project, another important part is operating system. For different environments, the development tools and programming language we use are different. The mainstream operating system on the market today are Android and iOS.

3.2.1. Android Operating System

Based on the Linux open-source system architecture, Google introduced the Android operating system for smart devices. Android is very powerful. From its launch in 2008 to the present, Android is known to occupy the number one position in the global smartphone operating system market. In the following figure, shows the mobile operating system market share worldwide from Apr 2021 to Apr 2022.

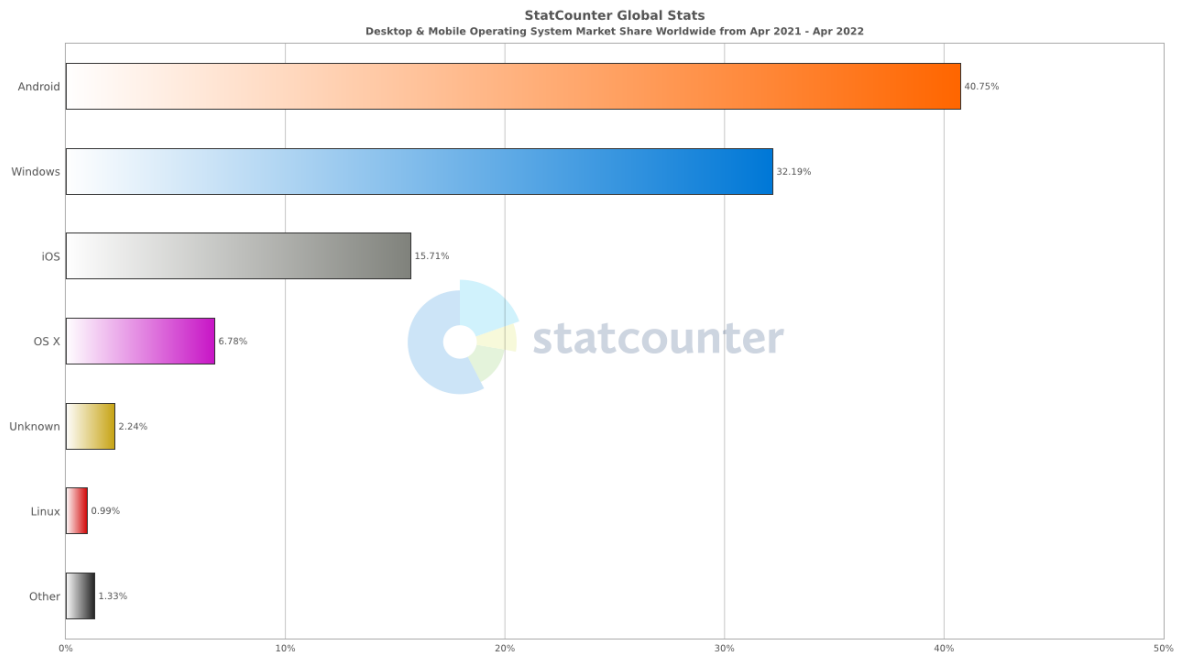


Figure 3.4. Operating System (source: statcounter)

Android can occupy such a large market share mainly because it has the following advantages:

- It is free and open-source development, which means that Android is completely free to use for developers and mobile phone manufacturers, reducing costs and increasing profits. Because the source code is open, it has attracted countless programmers from all over the world.
- The Android kernel is based on the Linux kernel and offers a wide range of APIs. The automation brought by API can easily save a lot of work, cost, and time.
- Allows program in Java, C or C++. And it allows applications multitask.

3.2.2. iOS Operating System

iOS is a mobile operating system for mobile devices of Apple, such like iPhone, iPad, and iPods. It is the second largest operating system after Android. Its advantages are smooth, stable, safe, and simple. In order to make the user experience better, iOS can be highly integrated with the hardware

system, so that electronic devices can respond in the shortest time. The background generated by iOS during use is pseudo background or no background program, and the degree of optimization is also very high. It rarely generates cache garbage files. When a software exits into the background, it will basically stop running, leaving space for other software in use, which makes the operation of iOS very process, rarely freeze phenomenon, in addition, the quality of iOS App is very high, the security is also very high, and it will not generate a lot of junk ads. Compare with android, the system's ability to adapt and the code's freedom account for the majority of the differences.

3.3. Reason for chosen

3.3.1. Overall scheme

In this project, we choose the wearable device to acquire human activity data, using the cell phone as the platform for information processing. Below, is a comparison of the parameter information of the cell phone and the wearable device.

Table 3.2 Performance comparison of smartphone and Hexiwear

	Smartphone (Redmi 9C)	Hexiwear
CPU	12nm process technology, up to 2.3GHz, 8x A53, octa-core CPU	Kinetis K64 32-bit Arm Cortex-M4 MCU, 120 MHz, 1M Flash, 256K SRAM
Battery	5000mAh	190mAh
Memory	64GB	8MB
Sensor	Accelerometer Proximity A-GPS	3D Accelerometer 3D Magnetometer 3-Axis Digital Gyroscope
Dimensions	164.9 x 77 x 9 mm	25.90 x 30.10 x 10 mm

With the above information, we can find out. Compared to Hexiwear, the smartphone has a higher power level and is able to work for a longer period of time. Likewise, smartphones have more computing power, can handle complex computing programs, and have enough storage space. But

the Hexiwaer is smaller and more portable than the smartphone, and has more sensors to capture human activity data.

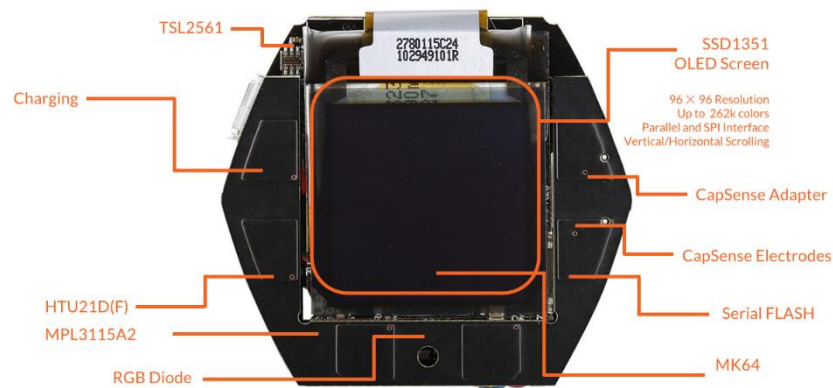
3.3.2. Hardware

For the hardware part, we choose Hexiwear as our wearable device. Although Xsens Dot can collect very accurate human motion data, it needs to wear multiple sensors at the same time during use, which is also very troublesome in the later data processing. Although Blue trident is convenient to use, there is no way to design programs according to the needs of users, the scalability is low, and the price is high.

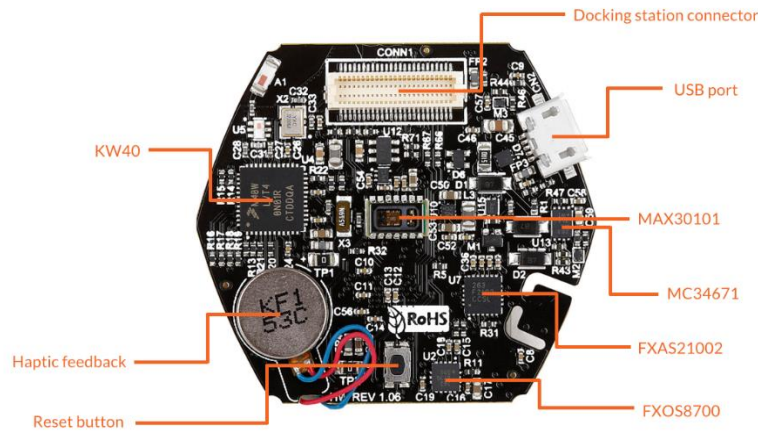
For Hexiwear, except 9-axis sensor, it has pulse oximeter and hear rate sensor, which giving us more choices. And Hexiwear is compatible with various external gadgets, and can use hundreds of sensors and transceivers with the Click board to enhance the core functions, allowing us to implement projects faster.

Secondly, compared with the other two wearable devices, Hexiwear's CPU processing power is more imposed, and its storage capacity and memory are much higher than the other two. This is very helpful for us to obtain data from the sensor later.

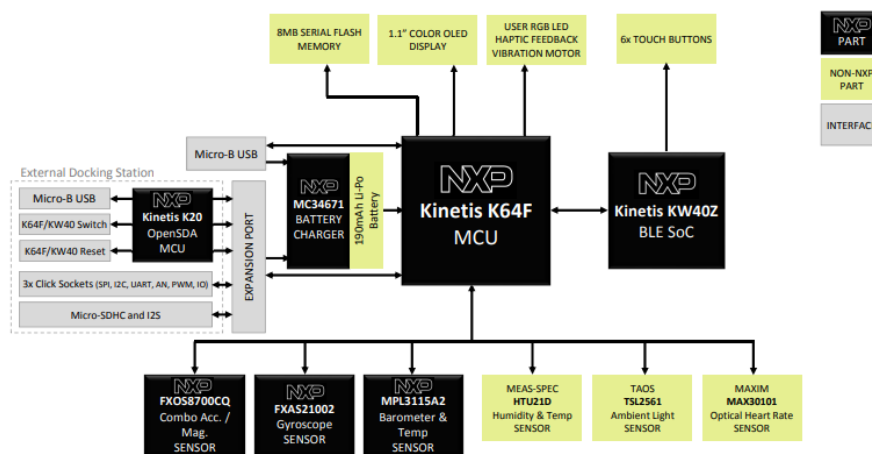
Finally, Kinetis Design Studio source files and complete hardware layouts and schematics are provided free of charge. We can refer to the existing projects of others to design the functions we want. Overall, Hexiwear is a very suitable choice compared to the other two wearable devices.



(a)



(b)



(c)

Figure 3.5. (a), (b) Hexiwear's PCB; (c) Hardware's block diagram. (source: MikroElektronika)

3.3.3. Software

As we mentioned before, the two most popular operating systems right now are Android and iOS. In this project, we choose to use Android Studio to develop the Android operating system. Android studio is an Android application development environment launched by Google. Different from Eclipse-based ADT, Android studio is a brand-new development environment with more powerful functions and more efficient performance. Using Android studio has the following advantages over using Eclipse development:

- Android studio only needs to add a line of configuration to use the v7 library and design library, and Eclipse needs to refer to the entire project to use these libraries.
- Higher versions of SDK and NDK only support Android studio, not Eclipse.
- More new functions are intelligently used in Android studio, such as automatic saving, multi-channel packaging, integrated version management, support for previewing drawable graphics files, etc.

Also, the available devices for testing were Android-powered phones, thus giving up on creating apps specifically for iOS.



Figure 3.6. Android Studio Log (source: android.com)

4. THEORETICAL BACKGROUND

4.1. Wireless communication

4.1.1. Low Energy Bluetooth 4.0 Overview

One of the most widely used short-range communication methods in the world is Bluetooth wireless communication technology. For Bluetooth 2.1+EDR, Bluetooth 3.0+HS and low energy Bluetooth 4.0, they all have the characteristics of close-range communication, low cost, robustness and can work license free in 2.4G RF. With the development of technology, the application of Bluetooth technology to games, cell phones, headsets, computers and other traditional areas can no longer meet the daily needs of people. The development of low energy Bluetooth has minimized the power consumption of devices, and is a new short-range wireless communication standard that combines traditional Bluetooth, high-speed Bluetooth, and low-power Bluetooth. Compared with the classic Bluetooth technology, low energy Bluetooth 4.0 mainly reduces power consumption from three aspects: (1) reduce standby power consumption; (2) fast connection; (3) reduce peak power

4.1.2. Low Energy Bluetooth 4.0 protocol stack

Low Energy Bluetooth 4.0 protocol stack is shown in the figure: the controller includes the Physical Layer (PHY), Link Layer (LL) and Host-Controller interface layer (HCI); the Host mainly includes the Logical Link Control and Adaption Protocol layer (L2CAP), Security Manager (SM), Attribute Protocol (ATT), Generic Access Profile (GAP), and Generic Attribute Profile (GATT); the Application layer is located in the upper layer of the controller and host. It belongs to the highest layer of Low Energy Bluetooth protocol, which defines three types: Characteristic, Service, and Profile.

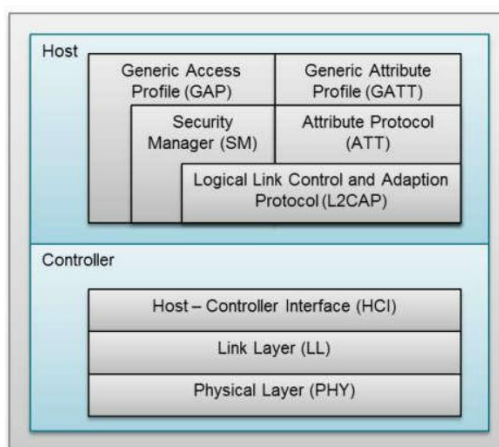


Figure 4.1. Low Energy Bluetooth Protocol Stack (source: Bluetooth Low Energy Software Developer's Guide)

4.1.3. Compare several short-range Wireless communication technologies

At present, in addition to Bluetooth communication technology, there are also ZigBee, Wi-Fi and other common wireless communication technologies. The following table shows a comparison of the technical parameters of wireless communication between the three.

Table 4.1 Compare several wireless communication technologies

Name	Wi-Fi	ZigBee	Bluetooth	BLE
Operating Frequency Band	2.4 GHz	2.4 GHz 868 MHz 915MHz	2.4 GHz	2.4 G
Limited speed	54 Mbps	250 kbps	3 Mbps	1 Mbps
Communication distance	100 m	10 – 60 m	10 m	50 m
Power consumption	10 – 50 mA	5 mA	30 mA	15 mA
Network topologies	Star network Mesh network	Star network Mesh network	Star network	Star network

4.2. Orientation

4.2.1. Represent Orientation

In the figure bellow, shows the orientation of Hexiwear. But in practice, the way we wear it is not necessarily the same as the picture below. In order to obtain the exact position of the human body in space, we need to re-represent the orientation. Currently, there are systems for representing orientations such as rotation matrices, Euler angles, quaternions, etc.

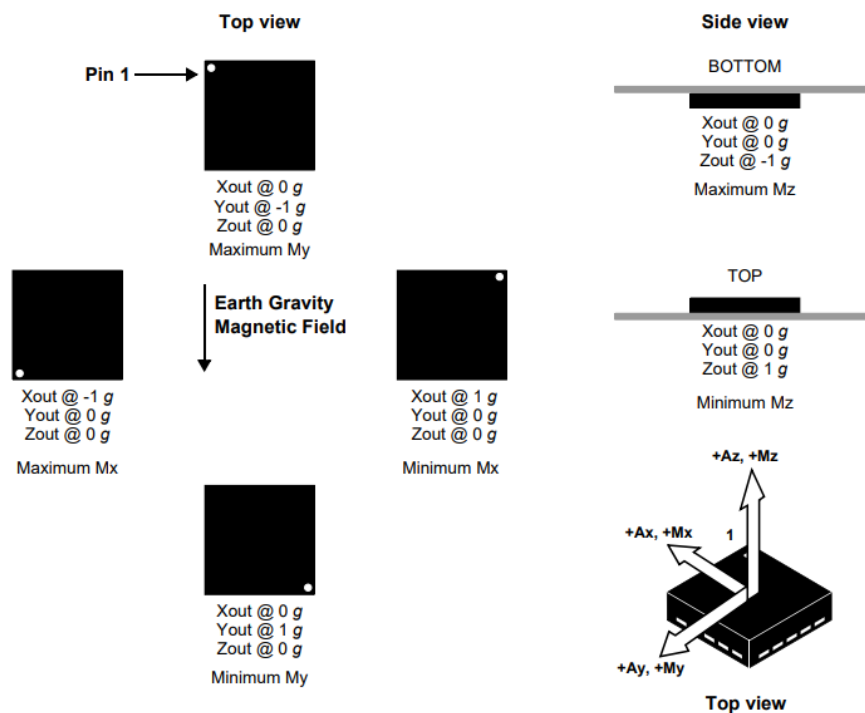


Figure 4.2. Hexiwear orientation and axis orientation (source: MikroElektronika)

4.2.1.1. Euler Angles

Euler Angle, which can represent 3 values in any direction in 3D space, was proposed by Leonhard Euler in the 18th century. The Euler angles we usually talk about can be subdivided into Euler-angles and Tait-Bryan-angles, both of which use the Cartesian coordinate system. The three axes are used as rotation axes, and the main difference lies in the selection order.

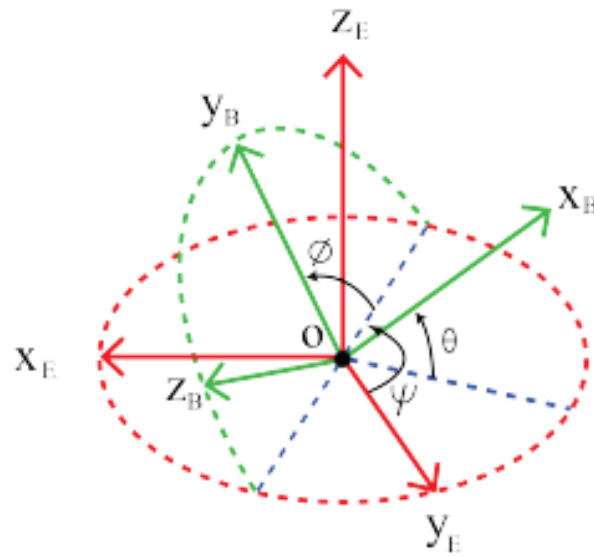


Figure 4.3. Tait-Bryan angles in Z-Y-X sequence (source: Yusheng [44])

4.2.1.2. Gimbal lock

A gimbal lock is a problem that arises when using dynamic Euler angles to represent the rotation of a 3D object. The usage of Euler angles is divided into static and dynamic. Static Euler angles are based on the world coordinate system (0,0,0); one of the definitions of dynamic Euler angles is the same as the static Euler angles, and the other is defined as follows: When using an object's coordinate system, When rotating in the XYZ mode, rotate in the following order: first around the X-axis, then around the Y-axis of the modified rigid body's right-hand coordinate system, and finally around the Z-axis of the twice-transformed rigid body's right-hand coordinate system.

- Static Euler angles: The rotation around the three axes of the world coordinate system is called static because the coordinate axis remains stationary during the rotation of the object.
- Dynamic Euler angles: The rotation around the three axes of the object coordinate system, because the coordinate axis rotates with the object in the same rotation process, so it is called dynamic.

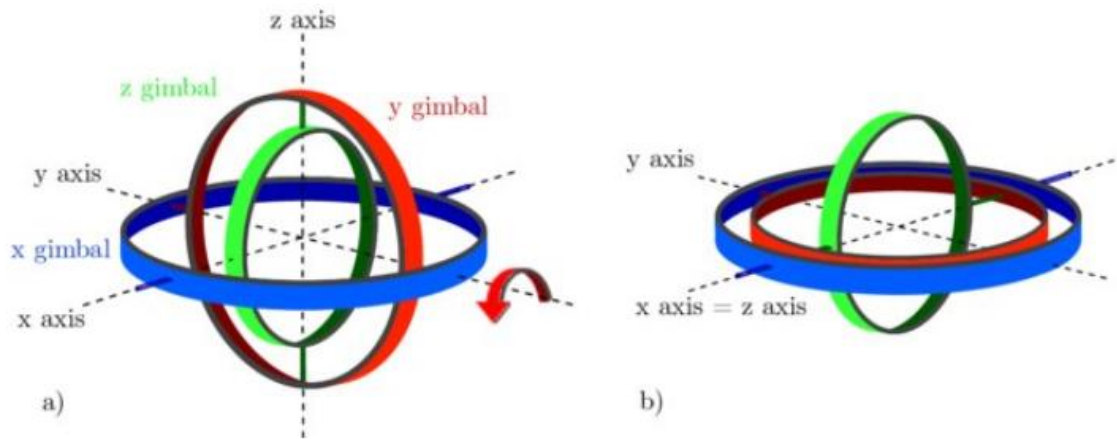


Figure 4.4. Gimbal lock (source: Julian Zeitlhöfler [29])

When $\pm 90^\circ$ is selected as the pitch angle, the first and third rotations become equivalent, and the rotation representation system as a whole is limited to merely rotating around the vertical axis, losing one representational dimension. A gimbal lock occurs when the second rotation, at an angle of $\pm 90^\circ$, causes the rotation axes of the first and third rotations to coincide.

4.2.1.3. Quaternions

In the previous section we explained the problem of gimbal locking in the Eulerian representation of the attitude, which leads to a problem when the Eulerian representation of the same spatial state is not unique, and when the gimbal locking phenomenon occurs, there are numerous Eulerian representations of the same rotation, which leads to a problem when the Eulerian angles differ. Because when the pitch angle is close to 90° , two completely different sets of Euler angular representations can be the same rotation. So, to solve these problems, the mathematics came up with a way to characterize the attitude in the form of quaternions.

The quaternion was invented by the Irish mathematician Hamilton. It is a combination of 1 scalar part and 3 vector part, which can usually be expressed as $\hat{q} = (q_1, q_2, q_3, q_4)$, where q_1 is the real number and q_2, q_3, q_4 are complex numbers.

Quaternions have the property of not allowing multiplication to be commutative. They are quite helpful for navigation as well as computer graphics and robotics applications. Starting from the work

of Mahony et al [36] and Madgwick et al introduced an orientation filter, which employs a quaternion representation of orientation [38][27].

$$Yaw = \text{atan2}(2q_2q_3 - 2q_1q_4, 2q_1^2 + 2q_2^2 - 1) \quad (\text{Eq. 4.1})$$

$$Pitch = -\sin^{-1}(2q_2q_4 + 2q_1q_3) \quad (\text{Eq. 4.2})$$

$$Roll = \text{atan2}(2q_3q_4 - 2q_1q_2, 2q_1^2 + 2q_4^2 - 1) \quad (\text{Eq. 4.3})$$

4.2.2. Measure of Orientation

To determine the direction of the human body during motion, we sometimes need to combine multiple sensors. The two prevailing mechanisms for obtaining direction are: Attitude and Heading Reference Systems (AHRS) and Inertial Measurement Units (IMU).

4.2.2.1. Attitude and heading reference system (AHRS)

Heading reference system, often known as AHRS (Attitude and Heading Reference System). AHRS consists of accelerometer, magnetometer and gyroscope, which can provide yaw, roll and pitch information for the aircraft. The Earth's gravity field, and consequently the Earth's field of force, serve as a key point of reference for AHRS, and the precision of these measurements determines the static ultimate accuracy of the system, whereas the gyroscope determines its dynamic performance. It implies that AHRS can't work properly once it leaves the gravity and magnetic field setting of the earth. We have to tendancy to special attention that the additional orthogonal the field of force and gravity field, the higher the aerial perspective measuring effect, that is to say, if the magnetic field and gravity field are parallel, such as at the north and south poles of the geomagnetic field, wherever the magnetic field is downward, that is, a similar direction because the weight field, this point the course intersection can not be measured, this is often the defect of the aerial attitude system, in high latitude places the course angle error can become larger and larger.

4.2.2.2. Inertial Measurement Units (IMU)

IMU (Inertial Measurement Unit) is the formal name for the mechanical phenomenon measurement unit. According to theoretical physics, all motion may be divided into two forms: linear motion and rotating motion. This inertial measurement unit is used to measure these two types of motion; linear motion can be measured using accelerometers, while rotational motion can be measured using gyroscopes. Three-axis accelerometers and three-axis gyroscopes are typically found in an IMU. While the gyroscopes capture the carrier's angular velocity signal relative to the navigation coordinate system, measure the object's angular velocity and acceleration in three-dimensional

space, and use it to determine the attitude of the solve object, the accelerometers capture the object's acceleration signal in the carrier coordinate system independently of the three axes. It is used in navigation for very important applications. To increase reliability, it is possible to equip each axis with additional sensors. The IMU is usually mounted in the center of gravity of the object to be measured.

IMUs are primarily used in devices that require motion control, such as cars and robots. They are also used in applications where an accurate derivation of displacement from position is required, such as inertial navigational systems for spaceships, missiles, submarines, and aircraft.

Assuming that the IMU gyroscope and accelerometer measurements are accurate, the gyroscope can accurately measure attitude of the object. The accelerometer can be quadratically integrated to derive the displacement to achieve full 6DOF, meaning that with a theoretical IMU at any position in the universe, we can know its current attitude and relative displacement, not restricted to a specific filed.

4.2.2.3. Algorithm

4.2.2.3.1 Gradient descent algorithm

The gradient descent algorithm was proposed by madgwick in 2010, and the figure below is from the madgwick paper. The core of the algorithm is to linearly fuse the pose obtained from accelerometer and magnetometer by gradient descent with the pose obtained from gyroscope integration to obtain the optimal pose. The advantage of the gradient descent algorithm is that the pose accuracy is higher than that of the complementary filtering algorithm.

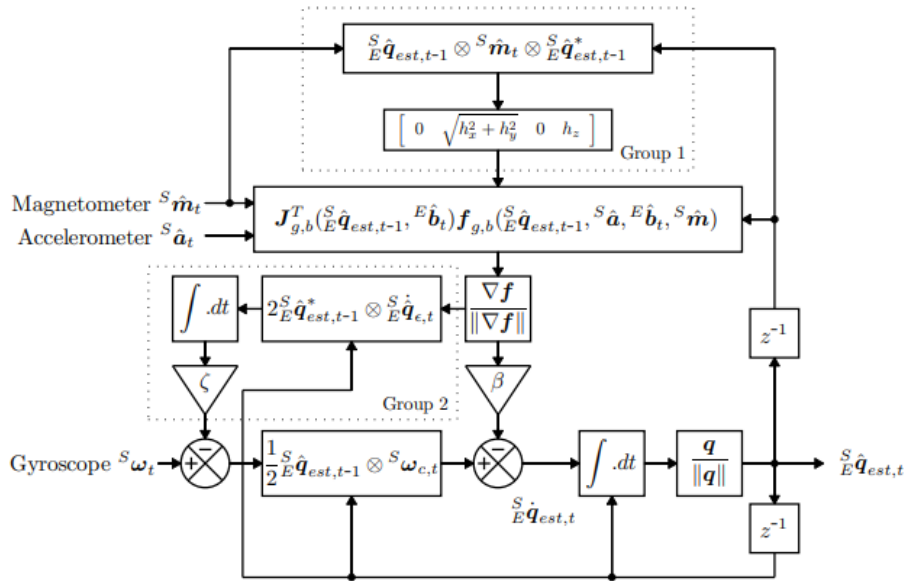


Figure 4.4. Madgwick's algorithm block diagram structure (source: madgwick internal report [39])

4.2.2.3.2 Explicit complement filter

The algorithm features a fusion solution using the complementary characteristics of the gyroscope, accelerometer and magnetometer outputs, which usually have high frequency characteristics, more sensitive when the carrier is moving at high speed, while the accelerometer and magnetometer are the opposite, with higher accuracy when the carrier movement is less variable.

Complementary filtering algorithm, through the PID feedback controller to the amount of error feedback compensation correction gyroscope error. Algorithm principle: According to the accelerometer and magnetometer data, after converting to the geographic coordinate system, and the corresponding reference gravity vector [37] and geomagnetic vector to find the fork product error, this error is used to correct the output of the gyroscope, and then use the gyroscope data for quaternion update, and then convert to Euler angles. In layman's terms, this means that the accelerometer output is used to correct the gyroscope's cross-roll and pitch angle errors [30], and the magnetometer output is used to correct the gyroscope's heading angle error, thus giving a smoother, slower dispersion attitude fusion result.



5. IMPLEMENTATION

In this chapter, we will explain the development of the prototype implementation. First, we will introduce how to implement the connection of the device, data collection and adjustments, then the processing and analysis of the data, and finally the overall experimental procedure.

5.1. Devices connect

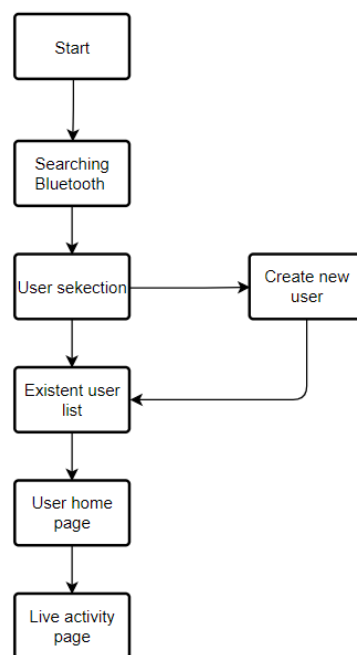


Figure 5.1. The block diagram of Algorithm

```

1. <?xml version="1.0" encoding="utf-8"?>
2. <manifest xmlns:android="http://schemas.android.com/apk/res/android"
3.     package="com.wolkabout.hexiwear">
4.
5.     <uses-permission android:name="android.permission.BLUETOOTH"/>
6.     <uses-permission android:name="android.permission.BLUETOOTH_ADMIN"/>
7.     <uses-permission android:name="android.permission.ACCESS_FINE_LOCATION"/>
8.
9. </application>
10. </manifest>
  
```

5.2. Data collection

5.2.1. Data collection

In the section 3.1 wearable devices, we introduced the main sensors that will be used. And we can find the motion service of those sensor. Figure 5.2 indicates the data format and the units of those sensor.

UUID	Characteristic	Format	Security Mode	R/W permissions	Details
0x2001	Accelerometer	int16_t[3]	Encryption with authentication	Read	Accel measurement for x, y, z coordinate. Range: +/- 4g
0x2002	Gyro	int16_t[3]	Encryption with authentication	Read	Gyro measurement for x, y, z coordinate. Range: +/- 256 deg/seg.
0x2003	Magnetometer	int16_t[3]	Encryption with authentication	Read	Magnet measurement for x, y, z coordinate.

Figure 5.2. Sensors used for measurement: FXOS8700CQ, FXAS21002 (source: MikroElektronika)

To get data from the sensor before, the application asks the wearable device for the eigenvalues service 0X2000.

5.2.2. Sample frequency

Sample frequency is an important parameter. From the point of view of the perspective of the transmitter, increasing the sampling rate can reduce the noise, reduce the difficulty of implementing RF output and improve signal transmission speed and bandwidth. From the point of view of the receiving end, although a high sampling rate can reduce quantization noise, it imposes a heavy load on subsequent digital signal processing, so it is necessary to reduce the sampling rate. In general, we should choose an appropriate sampling rate for the communication system. 100 HZ is a good choice.

5.3. Data treatment

When we get the raw data, we need to do the following processing on the data. As shown in the figure below. We first import the data from the CSV file and then use the MADGWICH algorithm to obtain the direction by means of quaternions. Finally, gravity compensation is given to the acceleration.

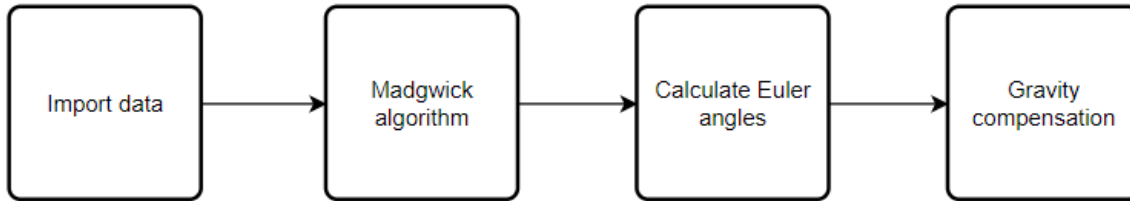


Figure 5.3. Data treatment block diagram.

5.3.1. Data import

Acceleration				Magnet			Gyroscope		
time	x	y	z	x	y	z	x	y	z
2022-04-24 16:47:54	0.84	-0.23	-0.50	30.90 μ T	16.20 μ T	95.10 μ T	36.00 $^{\circ}$ /s	-39.00 $^{\circ}$ /s	-10.00 $^{\circ}$ /s
2022-04-24 16:47:55	0.72	-0.04	0.05	21.90 μ T	18.10 μ T	66.10 μ T	-256.00 $^{\circ}$ /s	-256.00 $^{\circ}$ /s	92.00 $^{\circ}$ /s
2022-04-24 16:47:56	0.00	-0.03	-1.15	18.00 μ T	5.60 μ T	62.60 μ T	-256.00 $^{\circ}$ /s	-88.00 $^{\circ}$ /s	0.00 $^{\circ}$ /s
2022-04-24 16:47:57	0.54	-0.96	-0.30	45.90 μ T	1.70 μ T	107.50 μ T	-256.00 $^{\circ}$ /s	-63.00 $^{\circ}$ /s	217.00 $^{\circ}$ /s
2022-04-24 16:47:58	0.50	-0.32	-0.63	14.90 μ T	-6.30 μ T	78.00 μ T	145.00 $^{\circ}$ /s	253.00 $^{\circ}$ /s	-17.00 $^{\circ}$ /s
2022-04-24 16:48:00	0.96	-0.37	0.20	29.10 μ T	23.00 μ T	78.30 μ T	-39.00 $^{\circ}$ /s	-62.00 $^{\circ}$ /s	179.00 $^{\circ}$ /s
2022-04-24 16:48:01	0.77	-0.66	-0.41	38.00 μ T	30.90 μ T	70.50 μ T	85.00 $^{\circ}$ /s	71.00 $^{\circ}$ /s	11.00 $^{\circ}$ /s
2022-04-24 16:48:02	1.07	-0.45	-0.39	24.40 μ T	17.20 μ T	74.60 μ T	0.00 $^{\circ}$ /s	54.00 $^{\circ}$ /s	16.00 $^{\circ}$ /s
2022-04-24 16:48:03	0.96	0.06	-0.11	14.70 μ T	6.20 μ T	74.50 μ T	-4.00 $^{\circ}$ /s	-5.00 $^{\circ}$ /s	1.00 $^{\circ}$ /s
2022-04-24 16:48:04	1.01	-0.08	-0.20	17.50 μ T	13.10 μ T	80.30 μ T	-1.00 $^{\circ}$ /s	1.00 $^{\circ}$ /s	3.00 $^{\circ}$ /s
2022-04-24 16:48:05	0.99	-0.08	-0.24	17.20 μ T	12.50 μ T	84.40 μ T	2.00 $^{\circ}$ /s	-4.00 $^{\circ}$ /s	0.00 $^{\circ}$ /s
2022-04-24 16:48:06	1.02	-0.09	-0.28	16.90 μ T	14.30 μ T	78.00 μ T	-1.00 $^{\circ}$ /s	0.00 $^{\circ}$ /s	1.00 $^{\circ}$ /s
2022-04-24 16:48:07	0.99	-0.09	-0.20	18.90 μ T	13.10 μ T	80.80 μ T	-2.00 $^{\circ}$ /s	-1.00 $^{\circ}$ /s	1.00 $^{\circ}$ /s
2022-04-24 16:48:09	0.98	-0.12	-0.26	18.50 μ T	15.60 μ T	83.50 μ T	0.00 $^{\circ}$ /s	0.00 $^{\circ}$ /s	1.00 $^{\circ}$ /s

Figure 5.4. Raw data from Hexiwear.

5.3.2. Madgwick algorithm

We will utilize the Madgwick algorithm to define the gain and sampling period, two crucial filter parameters, after we get the data. Among them, we'll use a sampling frequency that matches the sensor's 60 Hz. In terms of gain, it is mostly the gyroscope measurement error in quaternion

derivative units. All errors, including noise, calibration mistakes, quantization errors, etc., are included in this parameter. The convergence ratio for removing these faults may be calculated from this value, therefore the higher, the faster the convergence and the bigger the error. In his study [40], the creator of this algorithm suggests that the ideal value of β to obtain good performance is 0.033 for IMU and 0.041 for MAGR. As a result, the recommended value is used since the MARG version was used in the project.

5.3.3. Calculate Euler angles

For further analysis, quaternions are so complex in their 4-D representation, it was decided to compute Euler angles. Therefore, Euler angles will be obtained by convention ZYX of quaternions.

5.3.4. Gravity compensation

Gravity compensation is the last data adjustment. According to Verasano [41] in his article, this modification is required to determine the coordinates of the real acceleration since without it, gravity would be at work. The author's suggested solution has been put into practice for this in the MATLAB programming language.

5.4. Data analysis

When we have finished processing the raw data, we will analyze the data.

By the Hexiwear device, we can obtain the acceleration A_x , A_y , A_z by accelerometer. In general, acceleration includes gravitational acceleration and linear acceleration. We will separate the acceleration force into gravitational acceleration and linear acceleration using a low-pass filter with a cutoff frequency of 0.25 Hz. So A_x will be split into G_{Ax} and L_{Ax} , and A_y and A_z will be treated the same way.

5.4.1. Feature Extraction

1) Signal Magnitude Vector

In the signal magnitude vector, we calculate for acceleration same for gyroscope,

$$A_{3a} = \sqrt{A_x^2 + A_y^2 + A_z^2} \quad (1)$$

$$LA_{3a} = \sqrt{LA_x^2 + LA_y^2 + LA_z^2} \quad (2)$$

$$G_{3a} = \sqrt{G_x^2 + G_y^2 + G_z^2} \quad (3)$$

$$GA_{3a} = \sqrt{GA_x^2 + GA_y^2 + GA_z^2} \quad (4)$$

2) Tilt angle (TA) of body trunk

TA is defined as the angle between the positive Ys and gravitational vector, as follows:

$$TA = \frac{LA_y}{\sqrt{LA_x^2 + LA_y^2 + LA_z^2}} \quad (5)$$

Therefore, we have twenty signals derived from the acceleration, angular velocity and orientation are listed as follows: $A_x, A_y, A_z, A_{3a}, GA_x, GA_y, GA_z, GA_{3a}, LA_x, LA_y, LA_z, LA_{3a}, G_x, G_y, G_z, G_{3a}, O_a, O_p, O_t$, and TA .

5.4.2. Feature selection

We will extract 140 features from acceleration, angular velocity and orientation according to the method of YI HE [41]. For example, A_xAvg represents the average value of LA_x . The remaining features are shown in the following table:

Table 5.1 Feature description

Features	Description
A_xAvg	The average value over the window of A_x
GA_xMed	The median value over the window of GA_x
LA_xStd	The standard deviation value over the window of LA_x
$G_{3a}SK$	The skewness value over the window of G_{3a}
O_aK	The kurtosis value over the window of O_a
O_pIR	The interquartile range over the window of O_p
O_tPD	The percentage of decline in the entire window of O_t

Where the Average means the average value over the window, Median means the median value over the window. Standard deviation means the standard deviation value over the window. Percentage of decline is the percentage of point decline in the entire window.

$$\text{Skewness: } SK = \frac{n}{(n-1)(n-2)} \sum \left(\frac{x_i - Avg}{Std} \right)^3 \quad (5)$$

$$\text{Kurtosis: } K = \frac{n(n+1) \sum (x_i - Avg)^4 - 3 \left(\sum (x_i - Avg)^2 \right)^2 (n-1)}{(n-1)(n-2)(n-3) Std^4} \quad (6)$$

$$\text{Interquartile range: } IR = Q_3 - Q_1 \quad (7)$$

Where Q_3, Q_1 is the 75th and 25th percentiles over the window, respectively.

5.5. Experimental procedure

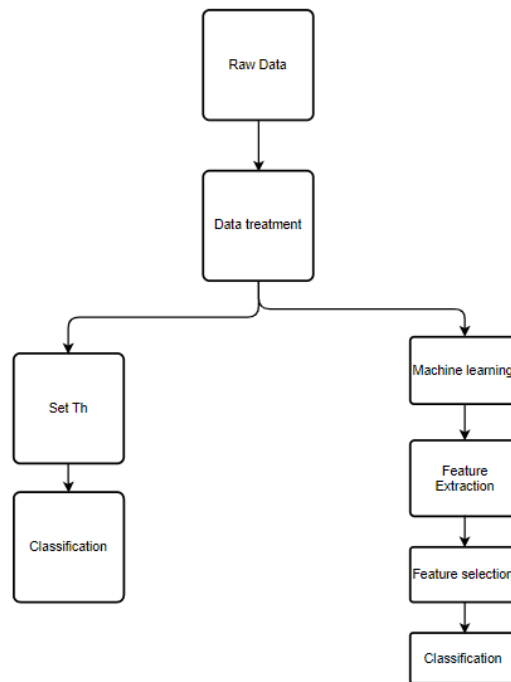


Figure 5.5. The framework of experimental procedure.

From the figure above, we see the stages in our overall experience. We first get the data through the wearable and then transmit the data to the mobile phone via Bluetooth. At this point, we will divide it into two steps, one of which is to display the current activity directly on the phone by setting a

threshold. The second is to send the device obtained by the mobile device to the computer via the mobile phone, and then use machine learning to determine the current activity. About setting thresholds. First, we partition the acceleration signal generated using T_{win} with 50% overlap. For each segment, A_{max} and A_{min} are used to specify the maximum and minimum acceleration values, respectively. Their times are T_{max} and T_{min} , respectively.

Our software mainly consists of three main screens, as shown in the image below.

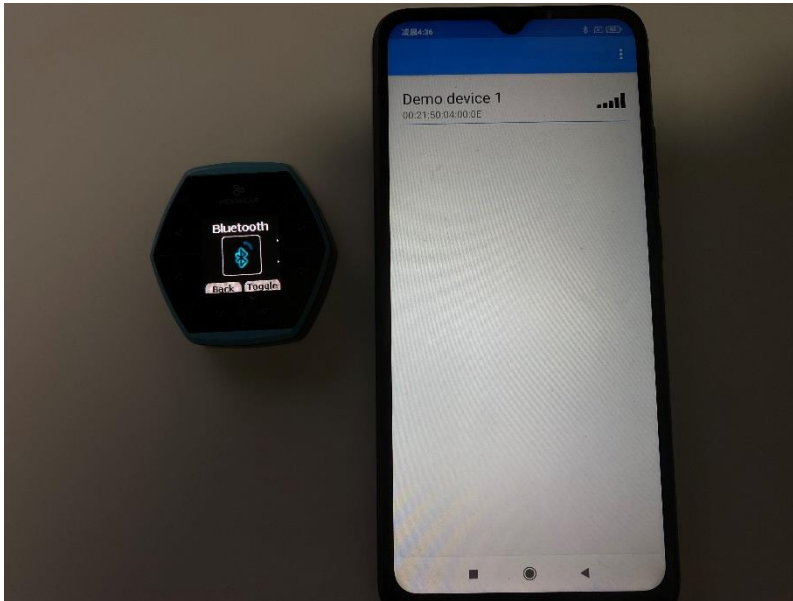


Figure 5.6. Screen to search for Bluetooth.

The first screen of our application, shown in Figure 5.6, is to search for Bluetooth devices near our smartphone.

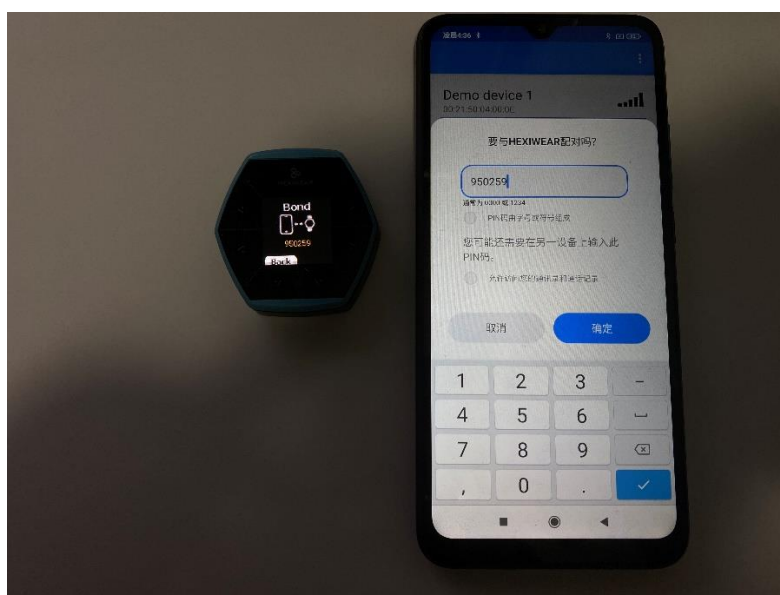


Figure 5.7. Screen to connect device.

The second screen is shown in Figure 5.7. It is to connect our smartphone and wearable device. Here we set a random connection password to connect the device correctly.

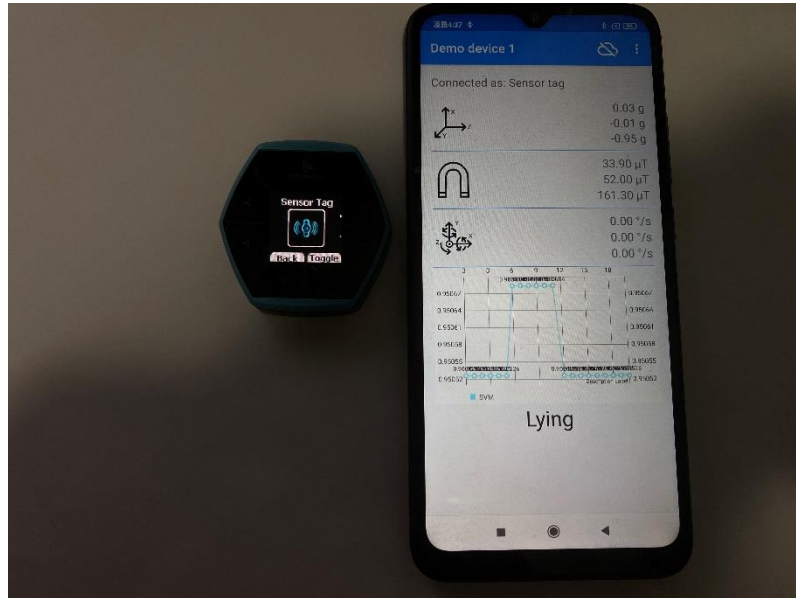
**Figure 5.8.** Screen of results.

Figure 5.8 shows our results. In the upper part, it is the acceleration value, magnetometer value, and gyroscope value collected by our Hexiwaer device. This is followed by a graph based on LA_{3a} . At the bottom is the current human activity detected by our algorithm based on the threshold.

6. RESULTS

In this section the results achieved in the project development are presented. It starts with an analysis of the different activities as well as a presentation of the demonstration and the final statistics of the results.

In the mobile application, we will take a simpler approach of threshold judgment since machine learning cannot be implanted. We divide the results into four major categories: vertical motion, horizontal motion, respectively. The horizontal motion is divided into sitting, standing, and lying. Vertical motion mainly contains falling, running, slow walking, etc.

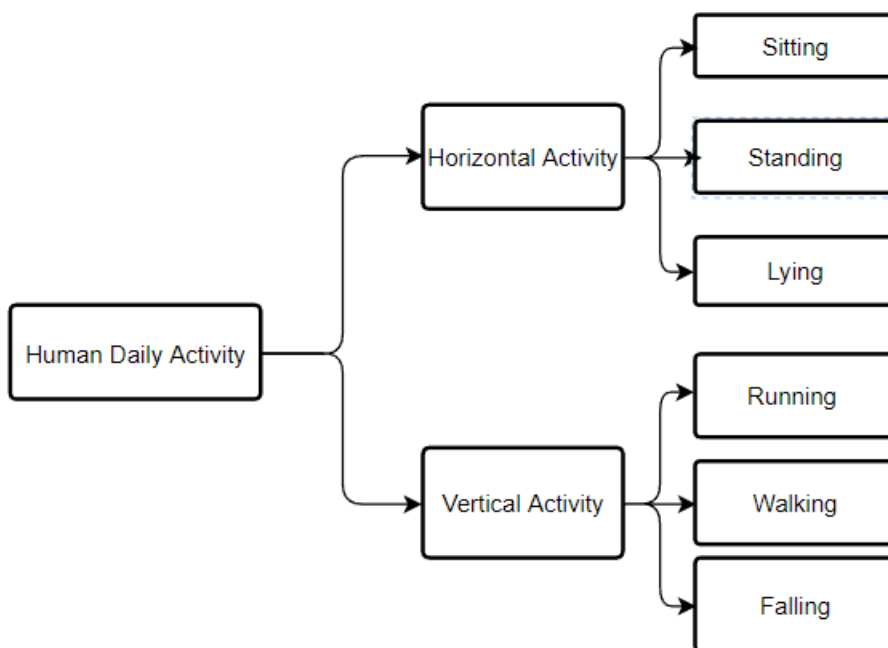


Figure 6.1. Classification of human daily activities.

6.1. Horizontal Activity

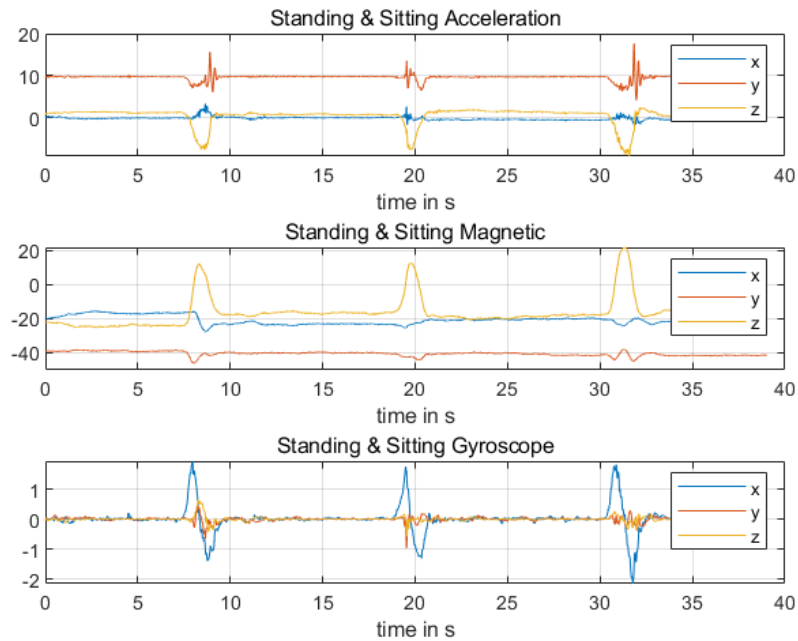


Figure 6.2. Plot the standing and sitting data from 3 different sensor of Hexiwear.

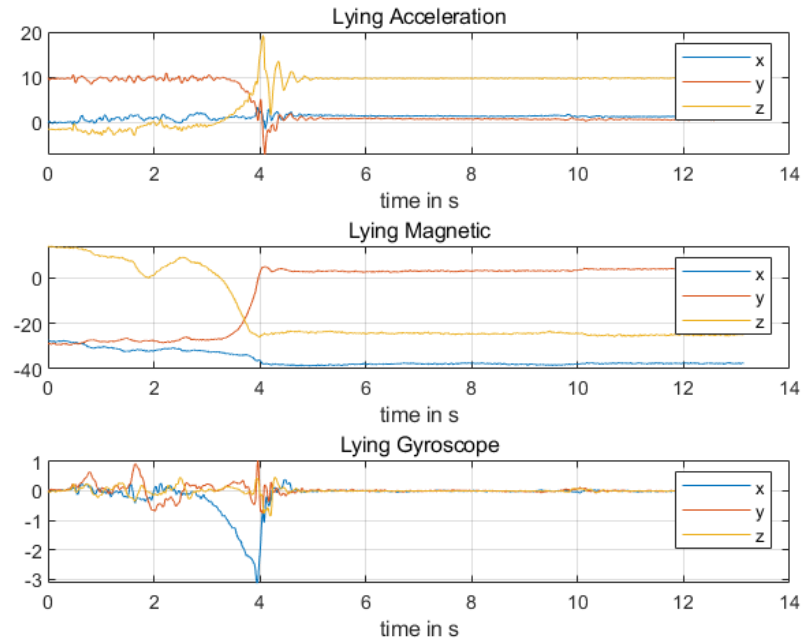


Figure 6.3. Plot the lying data from 3 different sensor of Hexiwear.

As we stated earlier, sitting, standing, and lying comprise the majority of horizontal activity. The activity data for sitting and standing are shown in Figure 6.2, and we can see that it is hard to distinguish between the two from the graphs. The activity data for lying are presented in Figure 6.3; in reality, there is really little variation between these three movements. The acceleration and

magnetometer information represent the biggest distinction between lying and the other two. The y-axis acceleration remains about 1 g whereas the z-axis and x-axis acceleration are both close to 0 g when they are sitting or standing. The z-axis acceleration is around 1 g while the x and y-axis acceleration are roughly equal to 0g when in the laying motion. Similar to it, there is a big difference in their magnetometer data.

6.2. Vertical Activity

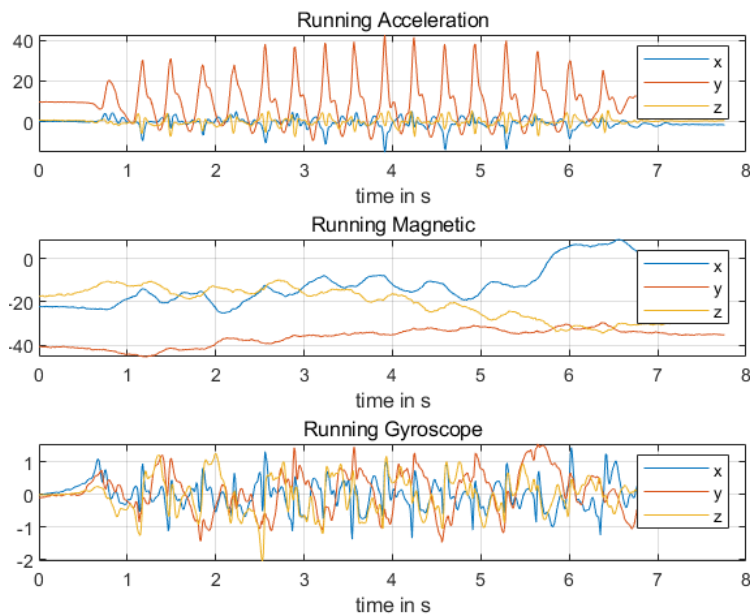


Figure 6.4. Plot the running data from 3 different sensor of Hexiwear.

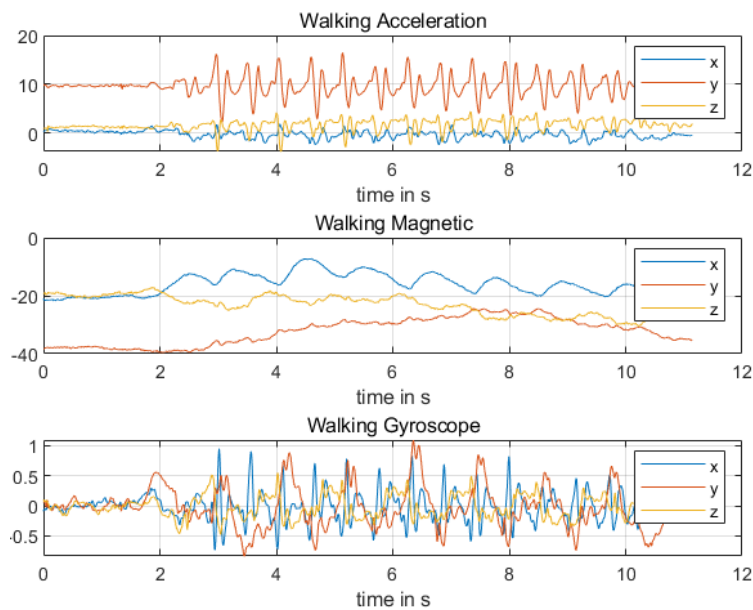


Figure 6.5. Plot the walking data from 3 different sensor of Hexiwear.

The two graphs up top show the activity data for walking and running, respectively. It is obvious that these two motion graphs share a similar overall pattern. While the peak y-axis acceleration for the walking motion is between 13 and 17 g, it exceeds 20 g for each peak for the running motion. The best method to differentiate between these two activities is with this one. Additionally, there are many more peaks for running than for walking at the same time, though the precise number varies on speed, the higher the speed, the larger the number.

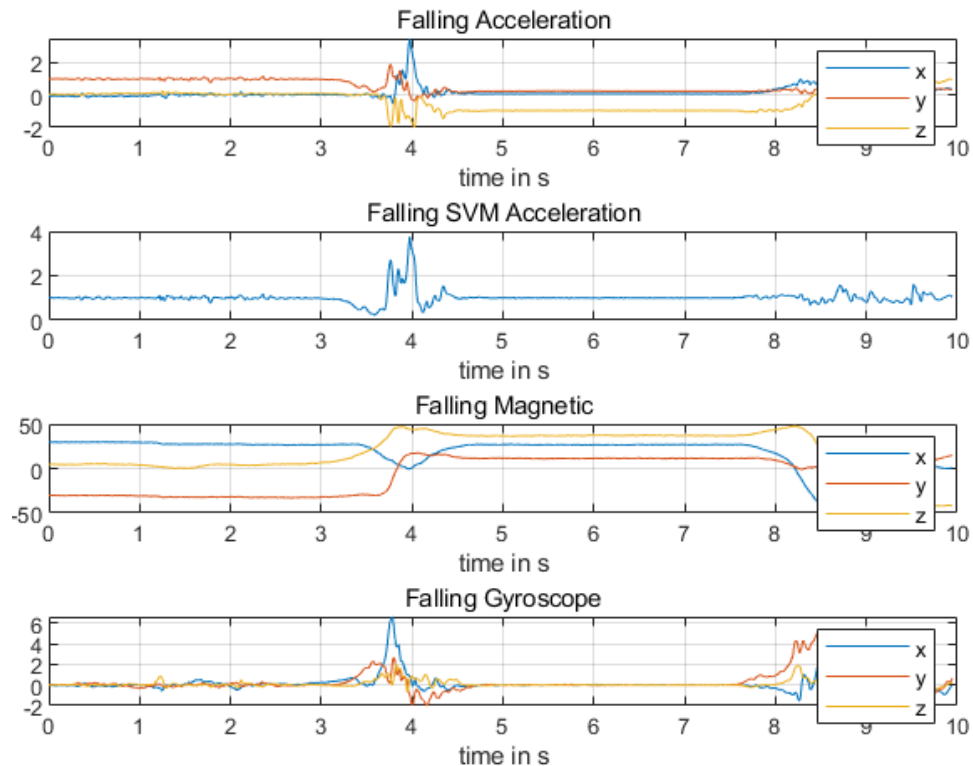


Figure 6.6. Plot the falling data from 3 different sensor of Hexiwear.

The graph of the curve during the fall is then displayed. We know that the change in acceleration throughout the fall process may be split into four phases, as Start, Impact, Aftermath, and Posture, according to Paola's study [43]. The RMS (Root Mean Square) of acceleration will usually be 0 g at the start of the fall process. After that, the RMS will quickly rise until it exceeds 2 g when the body hits with the ground or other objects. Following the impact, the body typically stays still for a brief amount of time, and during this time, the RMS normally levels off. The body will be moving in a different direction after the impact than it was before. Each axis' acceleration measurements will be different from what was observed before the fall.

6.3. Final Results

In this project, we did 50 repetitions of the experiment for each of the different human activities. The results obtained are shown in the following table.

Table 6.1 Experiment results

Activity	Test Times	Accuracy (%)
Sitting-Standing	70	95.71
Lying	70	97.14
Running	70	92.85
Walking	70	91.42
Falling	70	61.42

The above table shows that our system can accurately detect most of the human activities, but is less accurate in terms of falls. The main reason is that there are many different ways of falling in the process of falling, which can be mainly divided into forward fall, backward fall, and lateral fall. And in our experiments, the accuracy of forward falls is the highest, while the accuracy of lateral falls is the lowest.

In our testing process, we divide the test sites into two main categories: indoor sites with smooth roads and outdoor sites with uneven roads.

Activity	indoor sites with smooth roads	outdoor sites with uneven roads
Sitting-Standing	40	30
Lying	40	30
Running	40	30
Walking	40	30
Falling	40	30



7. CONCLUSIONS

7.1. Summary

In this project, we first studied the wearable devices available on the market that can record human activity, including their internal structure, the sensors they contain, inertial measurement units, etc.

Second, the Android Studio development environment was used to create a mobile application for the Android OS device. Through a low-power Bluetooth connection, this program can record data from the chosen hardware device and store it as a CSV file.

Finally, the information collected by the wearable device is fused to obtain multiple features, the effective features are filtered, the correlation between the features and human activity is found through machine learning, and the human activity can be predicted by the features.

Thus, the goals set in this project have been largely accomplished. This research makes use of expertise from a variety of domains, including signal processing, biomechanics, software engineering, etc.

7.2. Proposal and future work

Neither of the two methods used in this project yielded particularly perfect results. Methods of setting thresholds are limited by the fact that thresholds vary from tester to tester, and it is impossible to find a threshold that works for everyone. The thresholds we currently set may be very accurate for some people, but particularly inaccurate for another group of people. Our results are highly dependent on the wearer's position, requiring the wearer to be worn in the correct position in order to function, but this also sacrifices comfort and usability.

As for machine learning approaches, machine learning accuracy is much higher than thresholding methods. But it can only be implemented on computers, not smartphones yet. In the future, we plan to equip mobile phone applications with machine learning techniques to improve the accuracy of human activity detection.

8. ECONOMIC STUDY

The main cost of the project is the cost of material, licenses, and human resource. And also, we have added the personnel cost, it means we have paid for engineering hours costs. The engineer average hourly wage in Spain is 16 euros per hour [45]. And the planned completion time for our project is 750 hours.

Table 8.1 Cost of materials and licenses

Ref	Unit	Description	Price
1	1	Hexiwear	61,95 €
2	1	Hexiwear Docking Station	53,39 €
3	1	Hexiwear color pack	25,57 €
4	1	Alienware x15 R1	1.819,07 €
5	1	Redmi 9C	129,00 €
6	1	Android Studio	0 €
7	1	MATLAB	0 €
8	1	Microsoft Office	0 €
9	750	Engineer's salary	12000 €
		Total	14088,98 €

Table 8.2 Total cost of project

Concept	Amount
Total resources	14088,98 €
Non-direct costs (20%)	2817.79 €
Total	16906.77 €

BIBLIOGRAPHY

- [1] Wan S, Qi L, Xu X, Tong C, Gu Z. Deep Learning Models for Real-time Human Activity Recognition with Smartphones. *Mob Networks Appl.* 2020;25(2):743–55.
- [2] A.K. Bourke, C. Ni Scanail, K.M. Culhane, J.V. O'Brien and G.M. Lyons, "An optimum accelerometer configuration and simple algorithm for accurately detecting falls", *Proc. 24th IASTED Inter. Confer. BioEng.*, pp. 156-160, 2006.
- [3] A.K. Bourke, J.V. O'Brien and G.M. Lyons, "Evaluation of a threshold-based tri-axial accelerometer fall detection algorithm", *Gait & Posture*, pp. 194-199, 2007.
- [4] J. Chen, K. Kwong, D. Chang, J. Luk and R. Bajcsy, "Wearable Sensors for Reliable Fall Detection", *Proc. 27th Annu. Int. Conf. IEEE EMBS*, pp. 3551-3554, 2005.
- [5] M. Kangas, A. Konttila, I. Winblad and T. Jämsä, "Determination of simple thresholds for accelerometry-based parameters for fall detection", *Proc. 29th Annu. Int. Conf. IEEE EMBS*, pp. 1367-1370, 2007.
- [6] C. Wang, C. Chiang, P. Lin, Y. Chou, I. Kuo, C. Huang, et al., "Development of a Fall Detecting System for the Elderly Residents", *Proc. 2nd ICBBE*, pp. 1359-1362, 2008.
- [7] A. Purwar, D.U. Jeong and W.Y. Chung, "Activity Monitoring from Real-Time Triaxial Accelerometer data using Sensor Network", *Proc. 2nd ICBBE*, pp. 1359-1362, 2008.
- [8] P. Jantaraprim, P. Phukpattaranont, C. Limsakul and B. Wongkittisuksa, "Evaluation of Fall Detection for the Elderly on a Variety of Subject Groups", *Proc. 3rd I-CREAtE.*, pp. 42-45, 2009.
- [9] N. Noury, A. Fleury, P. Rumeau, A.K. Bourke, G.O. Laighin, V. Rialle, et al., "Fall detection – Principles and Methods", *Proc. 29th Annu. Int. Conf. IEEE EMBS*, pp. 1663-1666, 2007.
- [10] J. Edwards, "Wireless sensors relay medical insight to patients and caregivers [special reports]," *IEEE Signal Process. Mag.*, vol. 29, no. 3, pp. 8–12, May 2012.
- [11] K. Malhi, S. C. Mukhopadhyay, J. Schnepfer, M. Haefke, and H. Ewald, "A Zigbee-based wearable physiological parameters monitoring system," *IEEE Sensors J.*, vol. 12, no. 3, pp. 423–430, Mar. 2012.

- [12] Jin H, Huynh T P, Haick H. Self- healable sensors-based nanoparticles for detecting physiological markers via skin and breath: Toward disease prevention via wearable devices[J]. Nano Letters, 2016, 16(7):4194-4202
- [13] Rai P, Oh S, Shyamkumar P, et al. Nano-bio-textile sensors with mobile wireless platform for wearable health monitoring of neurological and cardiovascular disorders[J]. Journal of The Electrochemical Society, 2014, 161(2): B3116-B3150.
- [14] Mariani B, Jiménez M C, Vingerhoets F J, et al. On- shoe wearable sensors for gait and turning assessment of patients with Parkinson's disease[J]. IEEE Transactions on Biomedical Engineering, 2013, 60 (1): 155-158.
- [15] Maetzler W, Domingos J, Srulijes K, et al. Quantitative wearable sensors for objective assessment of Parkinson's disease[J]. Movement Disorders, 2013, 28(12): 1628-1637.
- [16] Cobelli C, Renard E, Kovatchev B P, et al. Pilot studies of wearable outpatient artificial pancreas in type 1 diabetes[J]. Diabetes Care, 2012, 35(9): e65-e67.
- [17] Cannon J G. Goodman and Gilman's the pharmacological basis of therapeutics. 11th edition[J]. Journal of Medicinal Chemistry, 2006, 49(3): 1222.
- [18] B. Mariani, M. C. Jiménez, F. J. G. Vingerhoets, and K. Aminian, "On-shoe wearable sensors for gait and turning assessment of patients with Parkinson's disease," IEEE Trans. Biomed. Eng., vol. 60, no. 1, pp. 155–158, Jan. 2013
- [19] B.-R. Chen et al., "A web-based system for home monitoring of patients with Parkinson's disease using wearable sensors," IEEE Trans. Biomed. Eng., vol. 58, no. 3, pp. 831–836, Mar. 2011.
- [20] S. Patel et al., "Monitoring motor fluctuations in patients with Parkinson's disease using wearable sensors," IEEE Trans. Inf. Technol. Biomed., vol. 13, no. 6, pp. 864–873, Nov. 2009.
- [21] Klucken J, Barth J, Kugler P, et al. Unbiased and mobile gait analysis detects motor impairment in Parkinson's disease[J]. PLOS ONE, 2013, 8(2): e56956.
- [22] Myo Naing Nyan, Francis Eng Hock Tay, Teck Hong Koh, Yih Yiow Sitoh and Kwong Luck Tan, "Location and sensitivity comparison of MEMS accelerometers in signal identification for ambulatory monitoring", Electronic Components and Technology, June 2004. Vol. 1, 1-4, Page(s):956-960.
- [23] J. M. Hausdorff, D. A. Rios, and H. K. Edelberg, "Gait variability and fall risk in community-living older adults: A 1-year prospective study," Archives of Physical Medicine and Rehabilitation, vol. 82, pp. 1050-1056, 2001.

- [24] W. H. O. Ageing and L. C. Unit, WHO global report on falls prevention in older age: World Health Organization, 2008.
- [25] KASTEREN T V, NOULAS A, ENGLEBIENNE G. Accurate activity recognition in a home setting[C]// International Conference on Ubiquitous Computing. ACM, 2008:1-9.
- [26] RAVI N, DANDEKAR N, MYSORE P, et al. Activity recognition from accelerometer data[C]// The Twentieth National Conference on Artificial Intelligence and the Seventeenth Innovative Applications of Artificial Intelligence Conference. DBLP, 2005:1541-1546.
- [27] Mourcou, Quentin, Anthony Fleury, Céline Franco, Frédéric Klopčič, and Nicolas Vuillerme. "Performance Evaluation of Smartphone Inertial Sensors Measurement for Range of Motion" , Sensors, 2015.
- [28] KHAN A M, LEE Y K, LEE S Y, et al. A triaxial accelerometer-based physical-activity recognition via augmented-signal features and a hierarchical recognizer[J]. IEEE Transactions on Information Technology in Biomedicine A Publication of the IEEE Engineering in Medicine & Biology Society, 2010, 14(5):1166-1172.
- [29] Zeitlhöfler, Julian. (2019). Nominal and observation-based attitude realization for precise orbit determination of the Jason satellites.
- [30] Nunzio Abbate, Adriano Basile, Carmen Brigante, Alessandro Faulisi, Fabrizio La Rosa. "Modern Breakthrough Technologies Enable New Applications Based on IMU Systems", Journal of Sensors, 2011
- [31] Hexiwear, "ARM MBED," [Online]. Available: <https://os.mbed.com/platforms/Hexiwear/>. [Accessed 20 04 2022]
- [32] MIKROE, "Complete IOT development solution," [Online]. Available: <https://www.mikroe.com/hexiwear>. [Accessed 20 04 2022]
- [33] Xsens, "Xsens Dot User Manual," [Online]. Available: <https://www.xsens.com/hubfs/Downloads/DOT/Documents/2021-07%20-%20Archived%20-%20Xsens%20DOT%20User%20Manual%20.pdf>. [Accessed 20 04 2022]
- [34] Blue Trident, "Blue Trident User Manual," [Online]. Available: <https://www.vicon.com/hardware/blue-trident/>. [Accessed 20 04 2022]
- [35] Novi Commentarii academiae scientiarum Petropolitanae 20, 1776, pp. 189–207

- [36] R. Mahony, T. Hamel and J.-M. Pflimlin, "Nonlinear complementary filters on the special orthogonal group", *IEEE Trans. Autom. Control*, vol. 53, no. 5, pp. 1203-1218, Jun. 2008.
- [37] Zheqi Yu, Adnan Zahid, Shuja Ansari, Hasan Abbas, Hadi Heidari, Muhammad A. Imran, Qammer H. Abbasi. "IMU Sensing–Based Hopfield Neuromorphic Computing for Human Activity Recognition" , *Frontiers in Communications and Networks*, 2022
- [38] A. M. Sabatini, "Quaternion-based extended Kalman filter for determining orientation by inertial and magnetic sensing", *IEEE Trans. Biomed. Eng.*, vol. 53, no. 7, pp. 1346-1356, Jul. 2006.
- [39] Madgwick, Sebastian. "An efficient orientation filter for inertial and inertial/magnetic sensor arrays." *Report x-io and University of Bristol (UK) 25 (2010): 113-118.*
- [40] S. O. H. Madgwick, A. J. L. Harrison and R. Vaidyanathan, "Estimation of IMU and MARG orientation using a gradient descent algorithm," *2011 IEEE International Conference on Rehabilitation Robotics*, 2011, pp. 1-7, doi: 10.1109/ICORR.2011.5975346.
- [41] Fabio Varesano. Simple gravity compensation for 9 DOM IMUs | Varesano.net. url: <http://www.varesano.net/blog/fabio/simple-gravity-compensation-9-dom-imus>
- [42] He, Yi, and Ye Li. "Physical Activity Recognition Utilizing the Built-In Kinematic Sensors of a Smartphone" , *International Journal of Distributed Sensor Networks*, 2013.
- [43] Paola Pierleoni, Alberto Belli, Lorenzo Palma, Marco Pellegrini, Luca Pernini, Simone Valenti. "A High Reliability Wearable Device for Elderly Fall Detection" , *IEEE Sensors Journal*, 2015
- [44] Sheng, Yu & Tao, Gang & Beling, Peter. (2019). Dynamic Mutation and Adaptive Tracking Control of Omni-Directional Multirotor Systems. 10.2514/6.2019-1562.
- [45] Salaryexplorer, "Engineer Average Salary in Spain 2022", [Online]. Available: <http://www.salaryexplorer.com/salary-survey.php?loc=203&loctype=1&job=261&jobtype=3>. [Accessed 27 09 2022]

